Neuron
Report

LRRTM2 Interacts with Neurexin1 and Regulates Excitatory Synapse Formation

Joris de Wit,[1] Emily Sylwestrak,[1,4] Matthew L. O'Sullivan,[1,4] Stefanie Otto,[1] Katie Tiglio,[1] Jeffrey N. Savas,[3] John R. Yates III,[3] Davide Comoletti,[2] Palmer Taylor,[2] and Anirvan Ghosh[1,*]
[1]Neurobiology Section, Division of Biology
[2]Department of Pharmacology, Skaggs School of Pharmacy and Pharmaceutical Sciences
University of California, San Diego, La Jolla, CA 92093, USA
[3]Department of Chemical Physiology, 10550 North Torrey Pines Road, SR11, The Scripps Research Institute, La Jolla, CA 92037, USA
[4]These authors contributed equally to this work
*Correspondence: aghosh@ucsd.edu
DOI 10.1016/j.neuron.2009.12.019

SUMMARY

We identify the leucine-rich repeat transmembrane protein LRRTM2 as a key regulator of excitatory synapse development and function. LRRTM2 localizes to excitatory synapses in transfected hippocampal neurons, and shRNA-mediated knockdown of LRRTM2 leads to a decrease in excitatory synapses without affecting inhibitory synapses. LRRTM2 interacts with PSD-95 and regulates surface expression of AMPA receptors, and lentivirus-mediated knockdown of LRRTM2 in vivo decreases the strength of evoked excitatory synaptic currents. Structure-function studies indicate that LRRTM2 induces presynaptic differentiation via the extracellular LRR domain. We identify Neurexin1 as a receptor for LRRTM2 based on affinity chromatography. LRRTM2 binds to both Neurexin 1α and Neurexin 1β, and shRNA-mediated knockdown of Neurexin1 abrogates LRRTM2-induced presynaptic differentiation. These observations indicate that an LRRTM2-Neurexin1 interaction plays a critical role in regulating excitatory synapse development.

INTRODUCTION

The function of the brain critically depends on appropriate synaptic connectivity. Specific patterns of connections, together with the properties of synaptic transmission at particular synapses, determine how the brain processes information. Although significant progress has been made in elucidating the pre- and postsynaptic organization of synapses, our understanding of the molecular mechanisms that regulate the development and function of CNS synapses is limited.

Synaptic cell adhesion molecules are key players in organizing synapse formation between appropriate synaptic partners. Hetero- or homophilic adhesive interactions across a nascent synapse allow target cell recognition and subsequent bidirectional differentiation of pre- and postsynaptic elements. Previous work has identified several synaptic cell adhesion molecules that can mediate *trans*-synaptic interaction to induce pre- and postsynaptic differentiation. These synaptogenic adhesion molecules include the neuroligins (Ichtchenko et al., 1995; Scheiffele et al., 2000; Song et al., 1999), synCAM (Biederer et al., 2002), NGL-2 and NGL-3 (Kim et al., 2006), and EphB2 (Kayser et al., 2006).

To identify novel transmembrane proteins that might regulate the development and function of synapses, we carried out an in silico screen for genes that showed subregion-specific expression in the adult hippocampus as reported in the Allen Brain Atlas (Lein et al., 2007) and encoded proteins with extracellular protein-protein interaction domains. Candidate genes were subsequently tested for putative synaptogenic properties in heterologous cell-neuron coculture assays (Biederer and Scheiffele, 2007; Scheiffele et al., 2000). This approach led to the identification of leucine-rich repeat transmembrane (LRRTM) proteins as proteins that could induce presynaptic differentiation. During the course of the study, Linhoff and colleagues reported that LRRTM proteins can induce synapse formation in hippocampal neurons (Linhoff et al., 2009), but several major questions remained unanswered. Importantly, whether endogenous LRRTMs contribute to synaptic function in vivo was not known, and the receptors that mediate the effects of LRRTM had not been identified. Here we provide evidence that endogenous LRRTM2 regulates excitatory synapse development and function in vitro and in vivo and identify Neurexins as functional receptors for LRRTM2.

RESULTS

LRRTM2 Regulates Excitatory Synapse Formation in Hippocampal Neurons

The *LRRTM* gene family consists of four genes, *LRRTM1–4*. Analysis of the *LRRTM* gene expression pattern by in situ hybridization showed that these genes are differentially expressed in the developing cortex and hippocampus (Figure S1). To determine the subcellular localization of LRRTM proteins, we transfected 293T cells with tagged constructs and examined their distribution by immunofluorescence. Myc-tagged LRRTM2–4 and LRRTM4L all localized to the cell membrane in transfected 293T cells (Figure S1). LRRTM1 however remained

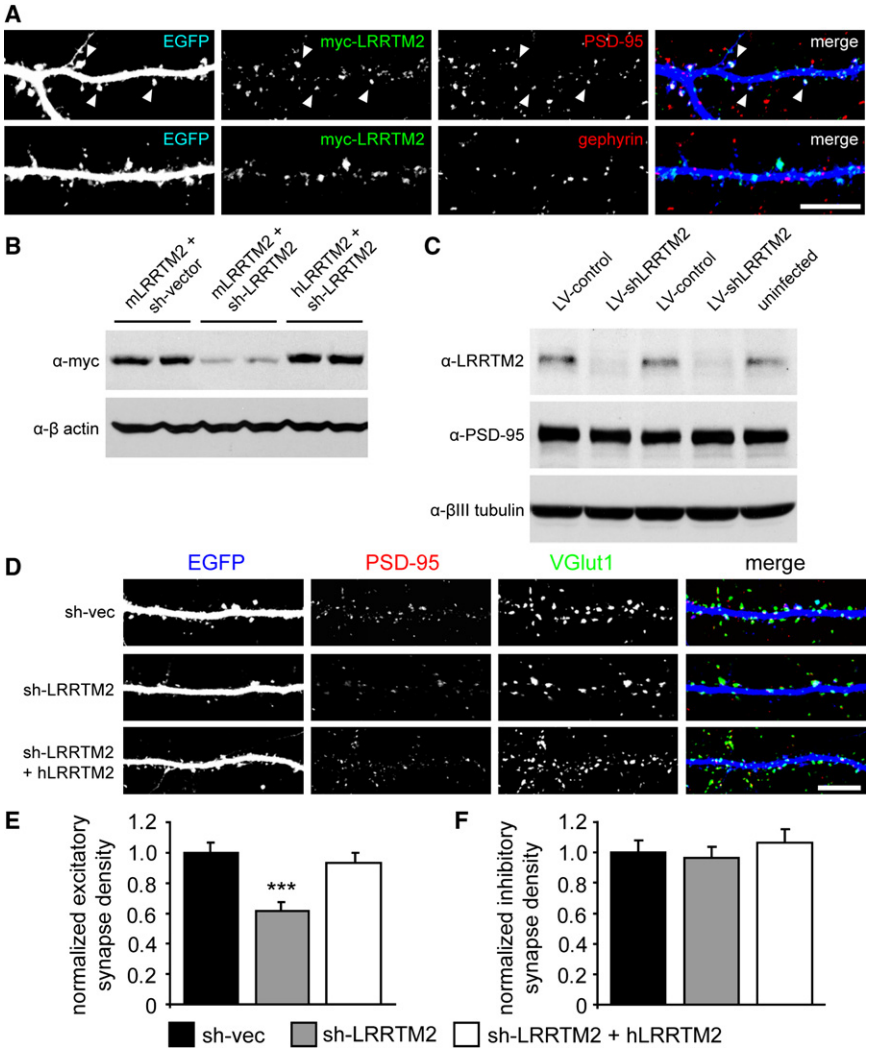

Figure 1. Knockdown of LRRTM2 Decreases Excitatory Synapse Density in Hippocampal Neurons

(A) Hippocampal neurons were cotransfected with myc-LRRTM2 and GFP at DIV 10 and immunostained for postsynaptic markers and GFP at DIV 17. Top panels, myc-LRRTM2 colocalizes with the excitatory postsynaptic marker PSD-95 in dendritic spines (arrowheads). Bottom panels, myc-LRRTM2 does not colocalize with the inhibitory postsynaptic marker gephyrin. GFP fluorescence shown in blue for better visualization. (B) 293T cells were cotransfected with mouse myc-LRRTM2 and the empty pSUPER vector (sh-vector) or pSUPER containing a shRNA against mouse and rat *LRRTM2* (sh-LRRTM2) for 48 hr. The LRRTM2 shRNA reduces expression of mouse LRRTM2 by 90%, but human myc-LRRTM2 is not affected. Samples were probed with a β-actin antibody to verify equal loading. (C) Knockdown of endogenous LRRTM2 in hippocampal neurons. Neurons were infected with control or sh-LRRTM2 containing lentiviral vectors (LV) at DIV 6 and analyzed at DIV 12. LRRTM2 protein levels are strongly reduced in LV-shLRRTM2-infected neurons compared to control infected or uninfected neurons. PSD-95 and βIII tubulin levels in the same samples are unchanged. (D) Hippocampal neurons were electroporated with the sh-vector (sh-vec), sh-LRRTM2, and sh-LRRTM2 with human myc-LRRTM2 (sh-LRRTM2 + hLRRTM2) and immunostained at DIV 14 for GFP, PSD-95, and VGlut1. (E) Quantification of the density of VGlut1/PSD-95-positive puncta per length of dendrite normalized to sh-vec control neurons. (***$p < 0.001$). (F) LRRTM2 knockdown does not affect inhibitory synapse density identified by VGAT/gephyrin colocalization. Scale bar in (A) and (D), 10 μm. Error bars represent SEM.

largely intracellular, despite the presence of a predicted transmembrane domain (Laurén et al., 2003), suggesting that LRRTM1 may require additional proteins for proper membrane targeting.

In a heterologous synapse induction assay, in which LRRTM proteins expressed in 293T cells were cocultured with hippocampal neurons, we found that LRRTM2 was more effective than the other *LRRTM* genes in inducing presynaptic differentiation (Figure S2). We therefore decided to investigate whether endogenous LRRTM2 contributed to synapse formation. To determine if LRRTM2 was targeted to excitatory synapses, hippocampal neurons were cotransfected with myc-tagged LRRTM2 and GFP and immunostained for synaptic markers. Myc-LRRTM2 clustered in the heads of dendritic spines, where it colocalized with the excitatory postsynaptic marker PSD-95, but not with the inhibitory postsynaptic marker gephyrin (Figure 1A). The quality of immunofluorescence with currently available LRRTM2 antibodies is not suitable to draw definitive conclusion about the localization of the endogenous protein, but the localization of the tagged proteins suggests that LRRTM2 primarily localizes to the postsynaptic density of excitatory synapses.

To examine the consequences of LRRTM2 loss of function, we generated an shRNA construct against LRRTM2 to knock down LRRTM2 expression in hippocampal neurons. The LRRTM2 shRNA reduced expression of myc-tagged mouse LRRTM2 in 293T cells by ~90% (Figure 1B). Myc-tagged human LRRTM2, which differs from mouse LRRTM2 by only one nucleotide in the shRNA target sequence, was not affected by the LRRTM2 shRNA, demonstrating target specificity (Figure 1B). To test the efficiency of sh-LRRTM2 in knocking down endogenous LRRTM2 protein levels in hippocampal neurons, the H1 promoter and shRNA were cloned into a lentiviral vector. Dissociated hippocampal neurons were infected at DIV 6, and cell lysate was analyzed by western blot on DIV 12. The LRRTM2 antibody (Figure S3) detects a weak band around 90 kDa in lysates of DIV 12 hippocampal neurons infected with the control virus, which was strongly reduced in neurons infected with the virus encoding the LRRTM2 shRNA (Figure 1C). Expression of sh-LRRTM2 did

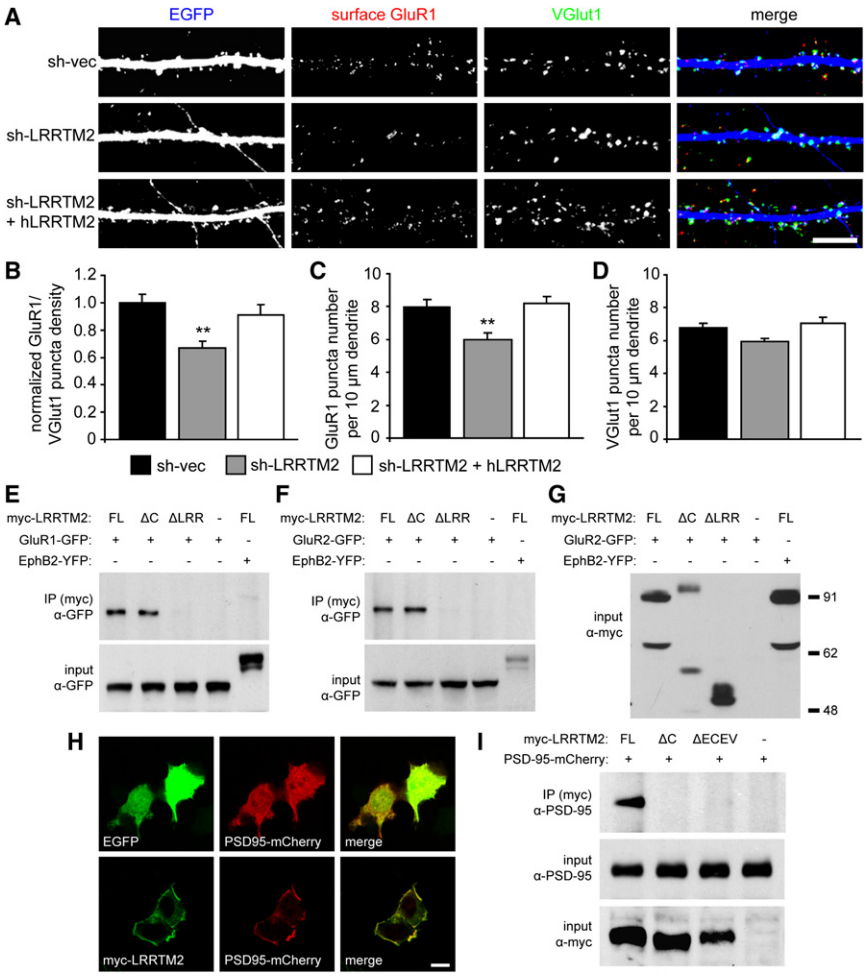

Figure 2. LRRTM2 Regulates GluR1 Surface Expression in Hippocampal Neurons and Interacts with Postsynaptic Proteins

(A) Hippocampal neurons were electroporated with the sh-vector (sh-vec), sh-LRRTM2, and sh-LRRTM2 with human myc-LRRTM2 (sh-LRRTM2 + hLRRTM2), surface labeled for GluR1, and immunostained at DIV 15 for GFP and VGlut1. (B) Quantification of the density of synaptic surface GluR1 puncta (VGlut1/GluR1 colocalization) per length of dendrite normalized to sh-vec control neurons (**$p < 0.001$). (C) Quantification of the GluR1 surface puncta per length of dendrite (**$p < 0.01$). (D) Quantification of the VGlut1 puncta per 10 µm dendrite. Bar graphs show mean ± SEM (difference not significant by ANOVA; $p = 0.02$ by Student's t test for control versus sh-LRRTM2). (E–G) 293T cells were cotransfected with myc-LRRTM2 mutant constructs and GluR1-GFP (E) or GluR2-GFP (F). Cell lysates were immunoprecipitated with myc antibodies and were analyzed by western blot using anti-GFP antibodies. EphB2-YFP was used as a negative control. A representative blot showing input samples probed with myc antibody is shown in (G). High and low molecular weight bands for LRRTM2 on western blot are probably due to glycosylation of LRRTM2. (H) Coexpression of PSD-95-mCherry with myc-LRRTM2 in 293T cells induces translocation to the cell membrane of PSD-95, which is diffusely distributed throughout the cytosol in GFP-expressing control cells. (I) Immunoprecipitation of myc-LRRTM2 deletion mutants lacking the cytoplasmic domain (LRRTM2 ΔC) or the C-terminal ECEV motif (LRRTM2 ΔECEV) coexpressed with PSD-95-mCherry in 293T cells. LRRTM2 interacts with PSD-95-mCherry via the ECEV motif. The high molecular weight band is shown for LRRTM2. Molecular weight markers in kDa indicated on the right. Scale bar in (A) and (H), 10 µm. Error bars represent SEM.

not affect protein levels of PSD-95 and βIII-tubulin in the same samples (Figure 1C).

To determine the effects of LRRTM2 knockdown on synapse development, we electroporated hippocampal neurons with LRRTM2 shRNA and control constructs and immunostained the cultures for the excitatory synapse markers PSD-95 and VGlut1 at DIV 14. Expression of sh-LRRTM2 in hippocampal neurons resulted in a 40% reduction in excitatory synapse density (Figures 1D and 1E), suggesting that endogenous LRRTM2 significantly contributes to excitatory synapse development. The decrease in excitatory synapse density following LRRTM2 knockdown was rescued by coexpression of human myc-LRRTM2 (Figures 1D and 1E), supporting target specificity of sh-LRRTM2. Expression of sh-LRRTM2 in hippocampal neurons had no effect on inhibitory synapse density (Figure 1F), indicating that expression of sh-LRRTM2 does not cause a general decrease in synapse density. These results indicate that endogenous LRRTM2 contributes to the development of excitatory, but not inhibitory, synapses in cultured hippocampal neurons.

LRRTM2 Regulates Surface Expression of GluR1-Containing Glutamate Receptors

The LRRTM2 loss-of-function studies suggest that LRRTM2 acts as a postsynaptic organizer of excitatory synapses in hippocampal neurons. A salient feature of hippocampal excitatory synapses is the presence of postsynaptic AMPA and NMDA receptors. To determine whether LRRTM2 recruits AMPA receptors to the postsynaptic density, we analyzed GluR1 surface expression following knockdown of LRRTM2. Neurons were electroporated with shRNA and control constructs, surface labeled for GluR1 at DIV 15, and subsequently permeabilized and immunostained for GFP and VGlut1. Knockdown of LRRTM2 resulted in a 33% decrease in the density of synaptic GluR1 surface puncta (Figures 2A and 2B). The decrease in density of synaptic GluR1 surface puncta following knockdown of LRRTM2 was rescued by coexpression of human LRRTM2 (Figures 2A and 2B). The reduction in synaptic GluR1 surface expression following LRRTM2 knockdown was caused primarily by a decrease in the density of GluR1 surface puncta (Figure 2C),

although the density of presynaptic VGlut1 puncta was also somewhat reduced (Figure 2D). This suggests that LRRTM2 acts as a postsynaptic organizer of the excitatory synapse and recruits AMPA receptors to the postsynaptic density.

To further investigate the interaction between LRRTM2 and glutamate receptors, we coexpressed myc-LRRTM2 together with GFP-tagged glutamate receptor subunits in 293T cells and examined their association by immunoprecipitation. Remarkably, GluR1-GFP, GluR2-GFP, and NR1-GFP all coprecipitated with full-length LRRTM2 (Figures 2E–2G and data not shown). Analysis of the LRRTM2 domain involved in glutamate receptor binding showed that LRRTM2 interacts with GluR1-GFP and GluR2-GFP via the LRR domain (Figures 2E–2G). EphB2-YFP did not coprecipitate with LRRTM2, indicating that coprecipitation with AMPA and NMDA receptor subunits does not reflect nonspecific interactions with transmembrane proteins. These data indicate that LRRTM2 can bind to glutamate receptor subunits via its extracellular LRR domain. Determination of whether endogenous LRRTM2 associates with glutamate receptors in vivo will require the development of suitable antibodies.

It is also possible that LRRTM2 recruits postsynaptic components via an interaction with synaptic scaffolding proteins. LRRTM proteins contain a highly conserved four amino acid sequence (ECEV) at their C terminus that is reminiscent of a PDZ-binding domain, suggesting that LRRTM2 might interact with PSD-95, an abundant PDZ-domain containing scaffolding protein (Sheng and Hoogenraad, 2007). Furthermore, several proteomic analyses of purified postsynaptic density fractions or immunopurified PSD-95 complexes have identified LRRTM1, LRRTM2, and LRRTM4 as constituents of the postsynaptic density (Dosemeci et al., 2007; Jordan et al., 2004; Yoshimura et al., 2004). To test whether LRRTM2 can interact with PSD-95, myc-tagged LRRTM2 was coexpressed with PSD-95-mCherry in 293T cells. In control cells expressing GFP, PSD-95-mCherry was distributed throughout the cytosol (Figure 2H). Upon coexpression of myc-LRRTM2, PSD-95-mCherry translocated to the cell membrane, where it colocalized with LRRTM2, indicating that LRRTM2 can recruit PSD-95 to the cell membrane (Figure 2H). To identify the domain of LRRTM2 that mediates binding to PSD-95, we generated LRRTM2 deletion constructs lacking the entire cytoplasmic domain (LRRTM2 ΔC) or the C-terminal four amino acids (LRRTM2 ΔECEV). Both LRRTM2 mutants were no longer able to bind PSD-95 in 293T cells (Figure 2I), indicating that the C-terminal ECEV motif in LRRTM2 mediates binding to PSD-95.

Loss of LRRTM2 Function In Vivo Leads to a Reduction in Glutamatergic Synaptic Transmission

To examine the role of LRRTM2 in synaptic function in vivo, we generated and stereotaxically injected lentiviruses expressing sh-LRRTM2 and GFP or a control vector into the dentate gyrus of P5–P6 rat pups. Hippocampal slices were cut between P13 and P16, and simultaneous recordings were made from uninfected and nearby infected dentate granule cells. A stimulating electrode placed in the outer half of the molecular layer was used to stimulate perforant path (PP) inputs onto granule cells (Figures 3A and 3B). No differences in cellular measures of integrity such as input resistance were found between treatment conditions (data not shown). Simultaneous recordings showed that knockdown of LRRTM2 in granule cells revealed a 58%

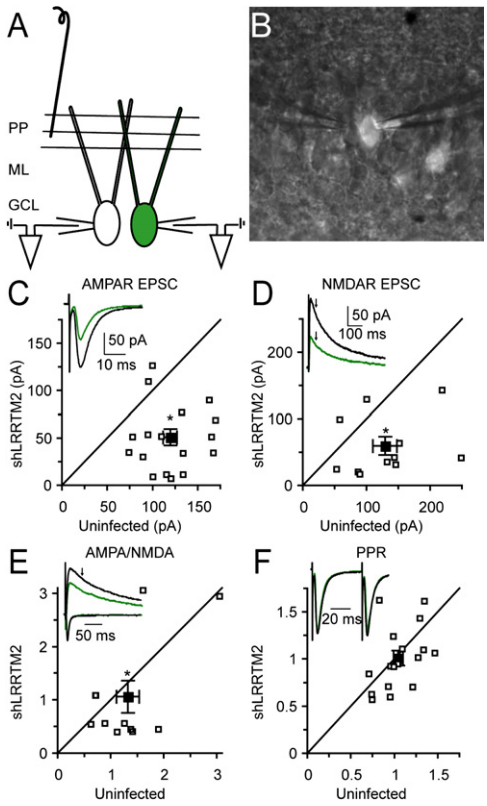

Figure 3. LRRTM2 Is Required for Excitatory Synapse Function In Vivo

(A) Schematic of experimental configuration. Rats were stereotaxically injected with lentivirus at P5, and acute slices were cut between P13 and P16. Whole-cell recordings were made from nearby infected and uninfected granule cells, identified by DIC and GFP epifluorescence, in the granule cell layer (GCL). Perforant path (PP) inputs were stimulated with an electrode in the outer half of the molecular layer (ML). (B) Overlaid GFP epifluorescence and DIC images of a simultaneous recording. (C) LRRTM2 shRNA causes a large reduction in AMPAR-mediated EPSCs (average AMPAR EPSC uninfected 119.5 ± 7.7 pA [mean ± SEM]: sh-LRRTM2 50.7 ± 8.5: n = 17 pairs, $p < 0.0001$). For all scatter plots, open symbols represent means from individual experiments and the filled symbol represents the group mean ± SEM. Inset: example average evoked PP AMPAR EPSCs recorded simultaneously from shLRRTM2 infected (green) and uninfected (black) GCs at a holding potential of −60 mV. (D) LRRTM2 shRNA causes a large reduction in NMDAR-mediated EPSCs (average NMDAR EPSC uninfected 129.0 ± 18.7 pA [mean ± SEM]: sh-LRRTM2 59.7 ± 13.5: n = 11 pairs, $p = 0.005$). Inset: example average evoked PP compound AMPAR- and NMDAR-mediated EPSCs recorded at a holding potential of +40 mV. Arrows indicate the time point 50 ms after the stimulus at which the NMDAR-mediated amplitude was measured. (E) LRRTM2 shRNA causes a slight reduction in AMPA/NMDA ratio (average PP AMPA/NMDA ratio uninfected 1.32 ± 0.21 [mean ± SEM]: sh-LRRTM2 1.06 ± 0.30: n = 11 pairs, $p = 0.04$). Inset: example average overlaid AMPAR and NMDAR EPSCs with traces scaled to the peak of the AMPAR EPSC. (F) LRRTM2 shRNA does not affect the paired-pulse ratio (PPR) of PP inputs onto GCs (averaged PP paired-pulse ratios uninfected 1.05 ± 0.06 [mean ± SEM]: sh-LRRTM2 1.01 ± 0.08: n = 17 pairs, $p = 0.54$). Inset: example average PP EPSCs from a simultaneous recording. Stimuli were delivered at 20 Hz. Traces are scaled to the peak of the first EPSC.

reduction in the strength of AMPAR-mediated EPSCs compared to neighboring uninfected cells (Figure 3C). In addition to AMPAR-mediated EPSCs, the strength of NMDAR-mediated PP inputs onto sh-LRRTM2-expressing granule cells was also significantly reduced by 54% (Figure 3D), indicating that endogenous LRRTM2 contributes significantly to excitatory synaptic transmission in vivo. LRRTM2 knockdown caused a small reduction in the ratio of AMPAR-mediated synaptic current to that carried by NMDARs (Figure 3E). LRRTM2 knockdown did not affect paired-pulse ratios (PPRs), a measure of presynaptic release probability, of the same inputs (Figure 3F). Infection with a control virus did not affect synaptic function by any of these measures (Figure S4). Together, these results demonstrate that loss of LRRTM2 function in vivo leads to a reduction in the glutamatergic transmission.

The reduction in evoked EPSCs in granule cells expressing sh-LRRTM2 could indicate a reduced number of synapses onto granule cells or a reduced glutamate receptor density at these synapses. To gain more insight in the consequences of loss of LRRTM2 in vivo, we recorded spontaneous AMPAR-mediated miniature excitatory postsynaptic currents (mEPSCs) from lentivirus-infected granule cells. Whole-cell recordings were made from infected cells, identified by GFP fluorescence, and AMPA mEPSCs were isolated pharmacologically. Analysis of AMPAR-mediated mEPSCs showed that loss of LRRTM2 in granule cells caused a small but significant decrease in mEPSC amplitude compared to control infected neurons (Figures S5A and S5B). The mEPSC frequency was not significantly affected in sh-LRRTM2-infected cells (Figure S5C). The decrease in mEPSC amplitude in sh-LRRTM2-infected granule cells indicates a reduction in strength of individual synapses and suggests that loss of LRRTM2 in hippocampal granule neurons reduces the density of postsynaptic AMPA receptors. The reduction in mEPSC amplitude, however, does not seem to be sufficient to account for the ~50% decrease in evoked synaptic currents (Figure 3), suggesting that LRRTM2 regulates both the efficacy of individual synapses and the number of synaptic inputs.

The Extracellular Domain of LRRTM2 Is Required for Its Synaptogenic Effect

To identify the domains of LRRTM2 that mediate its synaptogenic activity, we carried out gain-of-function experiments with full-length LRRTM2 and mutants that lack various domains. Overexpression of LRRTM2 in hippocampal cultures significantly increased the density of VGlut1/PSD-95-positive puncta along dendrites of transfected neurons compared to control neurons expressing GFP alone, indicating that LRRTM2 expression was sufficient to induce excitatory synapses (Figures S6A and S6B). In contrast, overexpression of LRRTM2 had no effect on the density of inhibitory synapses (Figures S6C and S6D).

To determine the relative contribution of the extra- and intracellular domains of LRRTM2 to excitatory synapse formation, hippocampal neurons were transfected with LRRTM2 deletion constructs lacking the intra- (LRRTM2 ΔC) or extracellular LRR (LRRTM2 ΔLRR) domains and immunostained for VGlut1 and PSD-95. Surface expression for all deletion mutant constructs was verified in 293T cells (data not shown). Overexpression of LRRTM2 ΔC resulted in a similar increase in excitatory synapse density as overexpression of full-length LRRTM2, but overexpression of the ΔLRR mutant abolished LRRTM2's synaptogenic effect (Figures 4A, S6E, and S6F). This indicates that the LRR domain is required for the LRRTM2-mediated increase in excitatory synapse density. Neutravidin beads coated with LRRTM2-ecto-Fc induced clustering of VGlut1 puncta in contacting neurites, indicating that the ectodomain is sufficient to induce presynaptic differentiation (Figure S6G). To determine whether the binding partner for LRRTM2 was localized to excitatory synapses, we incubated hippocampal cultures with clustered LRRTM2-ecto-Fc or control Fc, and examined the localization of LRRTM2 binding sites by costaining with anti-VGlut1 antibodies. LRRTM2-ecto-Fc and VGlut1 puncta were colocalized, suggesting that the LRRTM2 receptor is a synaptically localized protein (Figure S6H).

Neurexin1 Is a Functional LRRTM2 Receptor

The receptors for LRRTM proteins are not known. To identify the receptor for LRRTM2, we coupled LRRTM2-ecto-Fc or control Fc protein to proteinA beads, and column purified synaptosomal membrane proteins from P18 rat brains that bound Fc-LRRTM2. LRRTM2-associated proteins were then analyzed by MudPit tandem mass spectrometry (Washburn et al., 2001). We repeatedly found ~300 proteins to copurify with the ecto domain of LRRTM2 while fewer than 100 proteins copurified with Fc alone. Judging by the number of peptides and spectra hits, Neurexin family members were the most abundant proteins identified as potentially binding Fc-LRRTM2 (Figure 4B). We performed our screen with low (150 mM) and high (500 mM) salt washes, and under both conditions we found no Neurexin peptides in the Fc negative control, indicating a high level specificity in our assay (Table S1). Since many of the peptides are common to different Neurexin proteins, these results alone do not identify a unique Neurexin protein as the major binding partner, but strongly suggest that a Neurexin isoform is an LRRTM2 receptor.

To determine whether LRRTM2 binds to specific Neurexin family proteins, we performed a series of experiments to examine the binding of Fc-LRRTM2 to the surface of 293T cells expressing different Neurexin isoforms (Figures 4C–4F). 293T cells were transfected with the indicated isoforms, and 24 hr later the cells were exposed to clustered LRRTM2-ecto-Fc or control Fc proteins. Relative expression of Neurexin constructs is shown in Figure 4E. Following a 1 hr incubation, cultures were fixed and Fc binding assessed by immunofluorescence. As shown in Figures 4D and 4F, there was no significant LRRTM2 binding to control transfected cells (GFP, N-cadherin, NGL2). There was statistically significant binding to Neurexin 1α, but not Neurexin 2α or 3α. The highest level of binding was seen with Neurexin 1β (Figures 4D and 4F).

Neurexin 1β contains only one extracellular LNS domain that has previously been implicated in its interaction with Neuroligin. To determine whether the LNS domain of Neurexin 1β was specifically required for binding to LRRTM2, we tested two additional constructs in which the LNS domain of Neurexin 1β was replaced by the corresponding domain from Neurexin 2 or

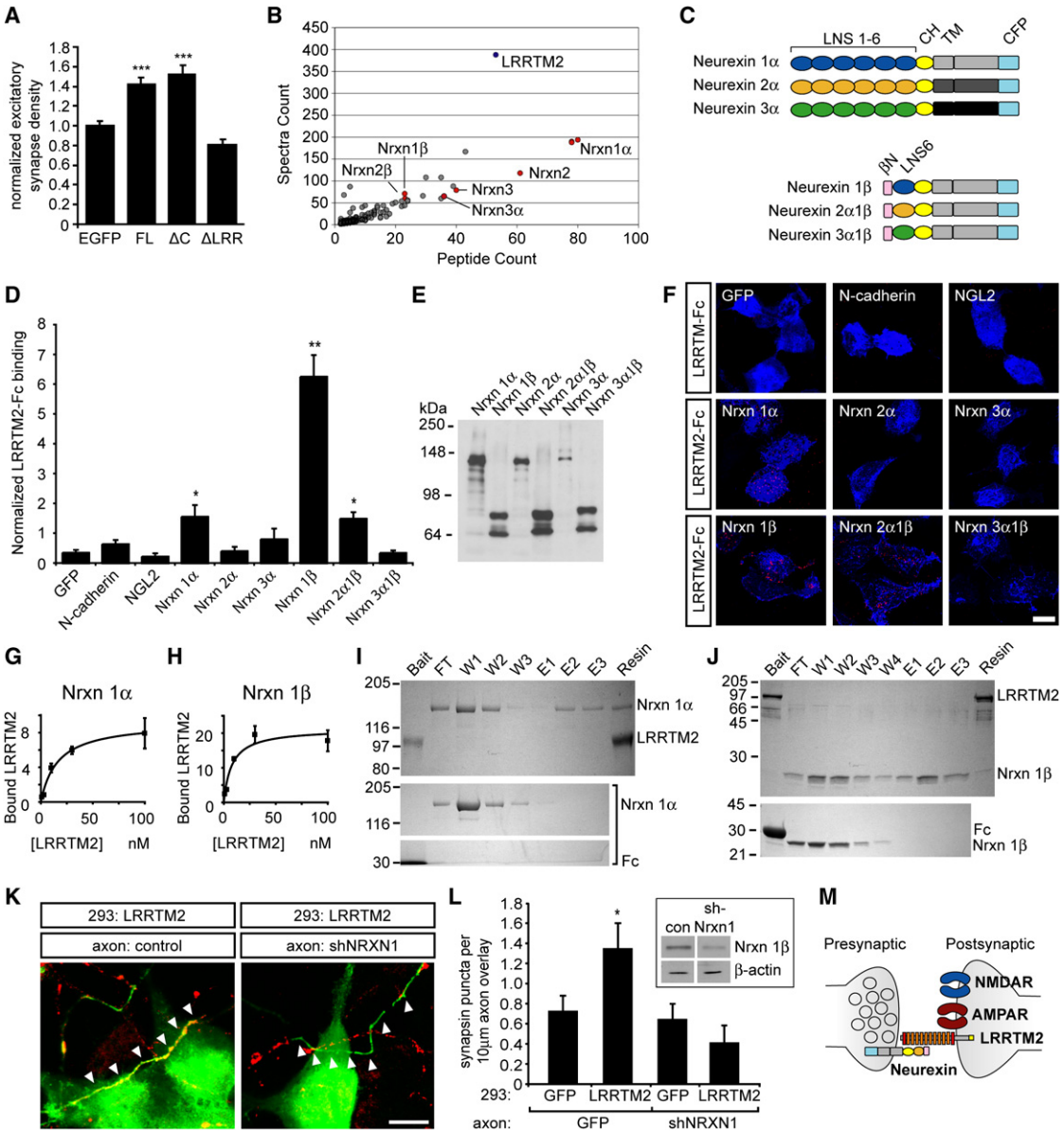

Figure 4. Neurexins Are Functional LRRTM2 Receptors

(A) LRRTM2 FL and LRRTM2 ΔC expressed in hippocampal neurons significantly increase excitatory synapse density (normalized excitatory synapse density) (***$p < 0.001$; ΔLRR not significantly different from controls by ANOVA, but $p = 0.01$ for pairwise comparison with control by Student's t test). See Figure S6E for accompanying fluorescence images. (B) Mass spec interaction screen identifies Neurexins as potential LRRTM2 receptors. The scatter plot is a graphical representation of a representative interaction screen. Each dot represents a protein that was identified by tandem mass spectrometry. The blue dot is LRRTM2 (bait protein), while the red dots are Neurexin family members. Gray dots represent other proteins that were also identified. The x axis represents the number of peptides and the y axis is the number of spectra in which the identified protein was found. (C) Schematic representation of Neurexin constructs. Neurexins (Nrxn) 1α, 2α, 3α, and 1β refer to the wild-type proteins. Nrxn 2α1β and Nrxn 3α1β are chimeric proteins of Nrxn1β with the LNS6 domain replaced with that of 2α and 3α, respectively. LNS, laminin, neurexin, sex-hormone-binding protein; CH, highly glycosylated region; βN, β specific leader; TM, transmembrane domain. All constructs have a C-terminal CFP tag. (D) Relative binding of LRRTM2-ecto-Fc to 293T cells expressing either Neurexins or control constructs. LRRTM2-Fc binds preferentially to 293T cells expressing Nrxn 1α, 1β, and 2α1β (*$p < 0.05$, **$p < 0.005$). All samples were normalized to an Fc-only control. (E) Relative expression of Neurexin-CFP constructs expressed in 293T cells, detected on western blot with anti-GFP antibody. (F) Confocal images of LRRTM2-ecto-Fc binding (red) to 293T cells (blue) expressing either Neurexin-CFP or control constructs. The CFP tag on neurexin constructs is pseudocolored blue to facilitate visualization of binding. Scale bar, 20 μm. (G) Binding of LRRTM2-ecto-Fc to Neurexin 1α-expressing 293T cells as a function of LRRTM2 concentration. (H) Binding of LRRTM2-ecto-Fc to Neurexin 1β-expressing 293T cells as a function of LRRTM2 concentration. (I and J) Direct binding of purified Neurexin 1α and 1β to immobilized LRRTM2-ecto-Fc. SDS-PAGE stained with Coomassie blue was used to separate the purified recombinant LRRTM2-ecto-Fc and either Neurexin 1α or 1β. Molecular weight standards, in kDa, are on the left. Proteins bands are identified on the right. FT, flow through of either Neurexin 1α (I) or Neurexin 1β (J). W1 through W4, washes; E1 through E3, elutions. Lack of binding to Fc control protein (E1–E3) is shown at bottom. Bait

Neurexin 3. The Neurexin 2α1β construct showed significant but highly reduced binding compared to Neurexin1β, whereas the Neurexin 3α1β construct showed no specific binding (Figures 4D and 4F). Consistent with a ligand-receptor relationship, Neurexins and LRRTM2 appear not to interact in *cis*, as they did not coprecipitate when coexpressed in 293T cells (data not shown). These results indicate that Neurexin 1α and Neurexin 1β are LRRTM2 receptors and that the LNS domain of Neurexin 1β is critical for its ability to bind LRRTM2.

To estimate the binding affinity of LRRTM2 to Neurexin 1α and 1β, we examined relative binding of LRRTM2 at various concentrations to 293T cells expressing Neurexin constructs. Scatchard plot analysis indicates LRRTM2 binding affinities as ~16 nM for Neurexin 1α and ~7 nM for Neurexin 1β (Figures 4G and 4H). It should be noted, however, that these represent affinities of LRRTM2 for Neurexin 1α and 1β expressed on the cell surface; an accurate intermolecular binding affinity would require analysis with recombinant purified proteins. To determine whether LRRTM2 directly binds to Neurexin 1α and 1β, we carried out a direct binding assay using recombinant LRRTM2 and Neurexin proteins. As shown in Figures 4I and 4J, both Neurexin 1α and 1β bound to LRRTM2-ecto-Fc immobilized on protein A beads and could be eluted from the column (lanes E2 and E3), indicating a direct interaction between these proteins.

Finally, to address whether Neurexin1 function was needed for LRRTM2-induced synaptic differentiation, we used the synapse induction assay in which 293T cells expressing LRRTM2 can induce presynaptic differentiation in cocultured hippocampal neurons (Figure S2). Hippocampal neurons were electroporated with either GFP or GFP together with an shRNA directed against Neurexin 1. At DIV 5, 293T cells expressing GFP alone or GFP + myc-LRRTM2 were overlayed on the neuronal culture. These cocultures were fixed and immunostained for GFP to visualize transfected axon/293T overlap and synapsin to identify presynaptic terminals, and the number of synaptic puncta per 10 μm of axon/293T overlap was quantified. As shown in Figures 4K and 4L, LRRTM2 induced presynaptic differentiation in control hippocampal axons. However, this effect was abolished in hippocampal neurons expressing shNrxn1, indicating that Neurexin1 function is necessary for LRRTM2-induced presynaptic differentiation.

DISCUSSION

The observations reported here identify LRRTM2 as a key regulator of excitatory synapse formation. LRRTM2 localizes to the postsynaptic density of excitatory synapses and induces functional presynaptic differentiation in contacting axons in coculture assays. A role for LRRTM2 in regulating postsynaptic differentiation is supported by the fact that LRRTM2 binds PSD-95 and regulates AMPA receptor surface expression, and knockdown of LRRTM2 in vivo decreases the strength of glutamatergic synaptic transmission without affecting presynaptic properties. Overexpression of LRRTM2 in cultured hippocampal neurons increases the density of excitatory synapses, without affecting inhibitory synapse density and knockdown of LRRTM2 in cultured neurons selectively decreases excitatory synapse density. Finally, we find that Neurexin1 acts as a functional receptor for LRRTM2. Neurexin 1α and 1β both show isoform-specific binding to LRRTM2, and knockdown of Neurexin1 blocks the ability of LRRTM2 to induce presynaptic differentiation. Together, these observations indicate that LRRTM2-Neurexin1 interactions play a critical role in the formation of excitatory synapses (Figure 4M).

Our observations suggest that LRRTM2 regulates postsynaptic function by interacting with key postsynaptic components. LRRTM2 interacts with PSD-95, and knockdown of LRRTM2 in dissociated neurons leads to a reduction in the density of PSD-95 puncta. Our data suggest that LRRTM2 can recruit PSD-95 to the postsynaptic density by binding to PSD-95 via the cytoplasmic ECEV motif in LRRTM2. The interaction of LRRTM2 with PSD-95 is significant, as PSD-95 plays an important role in regulating synaptic strength and plasticity by interacting with glutamate receptors and other synaptic signaling proteins (Kim and Sheng, 2004; Sheng and Hoogenraad, 2007; Han and Kim, 2008).

In further support of a postsynaptic role for LRRTM2, knockdown of LRRTM2 expression in cultured neurons strongly reduced synaptic GluR1 surface expression. This suggests that LRRTM2 recruits AMPARs to the postsynaptic density. One possibility is that LRRTM2 recruits AMPARs indirectly, through PSD-95 and TARPs (Chen et al., 2000; Schnell et al., 2002; Béïque et al., 2006; Elias et al., 2006). Alternatively, LRRTM2 could directly recruit AMPARs and NMDARs. We find that LRRTM2 can interact with AMPA and NMDA receptor subunits in heterologous cells via its extracellular domain, which suggests that one mechanism by which LRRTM2 promotes excitatory, but not inhibitory, synapse development could be through direct coupling with glutamate receptors in the postsynaptic membrane. This is an interesting possibility, but the interactions need to be confirmed for endogenous proteins.

In addition to regulating postsynaptic function, LRRTM2 is able to induce presynaptic differentiation. Our search for the presynaptic LRRTM2 receptor led to the identification of Neurexin 1α and 1β as LRRTM2 receptors. This is striking, as these Neurexins have previously been identified as the major receptors for Neuroligin1 (Dean et al., 2003; Ichtchenko et al., 1995), and Neuroligin1 has been widely studied as a regulator of excitatory synapse formation (reviewed in Craig and Kang, 2007; Südhof, 2008). Thus, it appears that neurexins function as receptors for two major classes of synaptogenic proteins. Finally, recent findings suggest that mutations in LRRTMs,

protein is LRRTM2-ecto-Fc. (K) Hippocampal neurons transfected with GFP (left) or GFP + shNRXN1 (right), cocultured with 293T cells expressing GFP + myc-LRRTM2. Cocultures were immunostained for GFP to identify axon/293T overlap and synapsin to identify presynaptic terminals. Arrowheads mark the trajectory of transfected axons. Note presence of synapsin puncta in control transfected axons (yellow) but not in shNrxn1-expressing axons. Scale bar, 10 μm. (L) Quantification of the experiment described in (K), showing that expression of shNrxn1 blocks the ability of LRRTM2 to induce presynaptic differentiation (*$p < 0.05$). Inset shows knockdown on Neurexin 1β, but not β-actin, in 293T cell lysates cotransfected with shNrxn1. (M) Model of regulation of excitatory synapse formation by LRRTM2-Neurexin1 interaction. Error bars represent SEM.

neuroligins, and neurexins are associated with autism and other neurological and psychiatric disorders (Majercak et al., 2006; Francks et al., 2007; Edwards et al., 2009; Südhof, 2008; Etherton et al., 2009). The identification of an LRRTM-Neurexin interaction as a key regulator of excitatory synapses should provide important insight into the molecular understanding of developmental cognitive disorders.

EXPERIMENTAL PROCEDURES

Please see Supplemental Data for details of experimental procedures.

SUPPLEMENTAL DATA

Supplemental Data include figures, a table, and Experimental Procedures and can be found with this article online at http://www.cell.com/neuron/supplemental/S0896-6273(09)01009-5.

ACKNOWLEDGMENTS

We thank members of the Ghosh lab for comments and helpful discussions and Richard Huganir (Glutamate receptors), Ann-Marie Craig (Neurexins), Matthew Dalva (EphB2-YFP), and Eunjoon Kim (NGL-2) for plasmids. This work was supported by a Rubicon Fellowship from the Netherlands Organisation for Scientific Research (NWO) (J.d.W.), NIH grant NS052772 (A.G.), and an Autism Speaks grant #2617 (D.C.).

Accepted: December 9, 2009
Published: December 23, 2009

REFERENCES

Béïque, J.C., Lin, D.T., Kang, M.G., Aizawa, H., Takamiya, K., and Huganir, R.L. (2006). Synapse-specific regulation of AMPA receptor function by PSD-95. Proc. Natl. Acad. Sci. USA *103*, 19535–19540.

Biederer, T., and Scheiffele, P. (2007). Mixed-culture assays for analyzing neuronal synapse formation. Nat. Protoc. *2*, 670–676.

Biederer, T., Sara, Y., Mozhayeva, M., Atasoy, D., Liu, X., Kavalali, E.T., and Südhof, T.C. (2002). SynCAM, a synaptic adhesion molecule that drives synapse assembly. Science *297*, 1525–1531.

Chen, L., Chetkovich, D.M., Petralia, R.S., Sweeney, N.T., Kawasaki, Y., Wenthold, R.J., Bredt, D.S., and Nicoll, R.A. (2000). Stargazin regulates synaptic targeting of AMPA receptors by two distinct mechanisms. Nature *408*, 936–943.

Craig, A.M., and Kang, Y. (2007). Neurexin-neuroligin signaling in synapse development. Curr. Opin. Neurobiol. *17*, 43–52.

Dean, C., Scholl, F.G., Choih, J., DeMaria, S., Berger, J., Isacoff, E., and Scheiffele, P. (2003). Neurexin mediates the assembly of presynaptic terminals. Nat. Neurosci. *6*, 708–716.

Dosemeci, A., Makusky, A.J., Jankowska-Stephens, E., Yang, X., Slotta, D.J., and Markey, S.P. (2007). Composition of the synaptic PSD-95 complex. Mol. Cell. Proteomics *6*, 1749–1760.

Edwards, T.L., Pericak-Vance, M., Gilbert, J.R., Haines, J.L., Martin, E.R., and Ritchie, M.D. (2009). An association analysis of Alzheimer disease candidate genes detects an ancestral risk haplotype clade in ACE and putative multilocus association between ACE, A2M, and LRRTM3. Am. J. Med. Genet. B Neuropsychiatr. Genet. *150B*, 721–735.

Elias, G.M., Funke, L., Stein, V., Grant, S.G., Bredt, D.S., and Nicoll, R.A. (2006). Synapse-specific and developmentally regulated targeting of AMPA receptors by a family of MAGUK scaffolding proteins. Neuron *52*, 307–320.

Etherton, M.R., Blaiss, C.A., Powell, C.M., and Südhof, T.C. (2009). Mouse neurexin-1alpha deletion causes correlated electrophysiological and behavioral changes consistent with cognitive impairments. Proc. Natl. Acad. Sci. USA *106*, 17998–18003.

Francks, C., Maegawa, S., Lauren, J., Abrahams, B.S., Velayos-Baeza, A., Medland, S.E., Colella, S., Groszer, M., McAuley, E.Z., Caffrey, T.M., et al. (2007). LRRTM1 on chromosome 2p12 is a maternally suppressed gene that is associated paternally with handedness and schizophrenia. Mol. Psychiatry *12*, 1129–1139.

Han, K., and Kim, E. (2008). Synaptic adhesion molecules and PSD-95. Prog. Neurobiol. *84*, 263–283.

Ichtchenko, K., Hata, Y., Nguyen, T., Ullrich, B., Missler, M., Moomaw, C., and Südhof, T.C. (1995). Neuroligin 1: a splice site-specific ligand for beta-neurexins. Cell *81*, 435–443.

Jordan, B.A., Fernholz, B.D., Boussac, M., Xu, C., Grigorean, G., Ziff, E.B., and Neubert, T.A. (2004). Identification and verification of novel rodent postsynaptic density proteins. Mol. Cell. Proteomics *3*, 857–871.

Kayser, M.S., McClelland, A.C., Hughes, E.G., and Dalva, M.B. (2006). Intracellular and trans-synaptic regulation of glutamatergic synaptogenesis by EphB receptors. J. Neurosci. *26*, 12152–12164.

Kim, E., and Sheng, M. (2004). PDZ domain proteins of synapses. Nat. Rev. Neurosci. *5*, 771–781.

Kim, S., Burette, A., Chung, H.S., Kwon, S.K., Woo, J., Lee, H.W., Kim, K., Kim, H., Weinberg, R.J., and Kim, E. (2006). NGL family PSD-95-interacting adhesion molecules regulate excitatory synapse formation. Nat. Neurosci. *9*, 1294–1301.

Laurén, J., Airaksinen, M.S., Saarma, M., and Timmusk, T. (2003). A novel gene family encoding leucine-rich repeat transmembrane proteins differentially expressed in the nervous system. Genomics *81*, 411–421.

Lein, E.S., Hawrylycz, M.J., Ao, N., Ayres, M., Bensinger, A., Bernard, A., Boe, A.F., Boguski, M.S., Brockway, K.S., Byrnes, E.J., et al. (2007). Genome-wide atlas of gene expression in the adult mouse brain. Nature *445*, 168–176.

Linhoff, M.W., Laurén, J., Cassidy, R.M., Dobie, F.A., Takahashi, H., Nygaard, H.B., Airaksinen, M.S., Strittmatter, S.M., and Craig, A.M. (2009). An unbiased expression screen for synaptogenic proteins identifies the LRRTM protein family as synaptic organizers. Neuron *61*, 734–749.

Majercak, J., Ray, W.J., Espeseth, A., Simon, A., Shi, X.P., Wolffe, C., Getty, K., Marine, S., Stec, E., Ferrer, M., et al. (2006). LRRTM3 promotes processing of amyloid-precursor protein by BACE1 and is a positional candidate gene for late-onset Alzheimer's disease. Proc. Natl. Acad. Sci. USA *103*, 17967–17972.

Scheiffele, P., Fan, J., Choih, J., Fetter, R., and Serafini, T. (2000). Neuroligin expressed in nonneuronal cells triggers presynaptic development in contacting axons. Cell *101*, 657–669.

Schnell, E., Sizemore, M., Karimzadegan, S., Chen, L., Bredt, D.S., and Nicoll, R.A. (2002). Direct interactions between PSD-95 and stargazin control synaptic AMPA receptor number. Proc. Natl. Acad. Sci. USA *99*, 13902–13907.

Sheng, M., and Hoogenraad, C.C. (2007). The postsynaptic architecture of excitatory synapses: a more quantitative view. Annu. Rev. Biochem. *76*, 823–847.

Song, J.Y., Ichtchenko, K., Südhof, T.C., and Brose, N. (1999). Neuroligin 1 is a postsynaptic cell-adhesion molecule of excitatory synapses. Proc. Natl. Acad. Sci. USA *96*, 1100–1105.

Südhof, T.C. (2008). Neuroligins and neurexins link synaptic function to cognitive disease. Nature *455*, 903–911.

Washburn, M.P., Wolters, D., and Yates, J.R., 3rd. (2001). Large-scale analysis of the yeast proteome by multidimensional protein identification technology. Nat. Biotechnol. *19*, 242–247.

Yoshimura, Y., Yamauchi, Y., Shinkawa, T., Taoka, M., Donai, H., Takahashi, N., Isobe, T., and Yamauchi, T. (2004). Molecular constituents of the postsynaptic density fraction revealed by proteomic analysis using multidimensional liquid chromatography-tandem mass spectrometry. J. Neurochem. *88*, 759–768.